I - 508

A CONCENTRATED PLASTICITY APPROACH TO WIND-INDUCED INELASTIC INSTABILITY ANALYSIS OF CABLE-STAYED BRIDGES

Virote BOONYAPINYO, Member, Yokohama National University
Toshio MIYATA, Member, Yokohama National University
Hitoshi YAMADA, Member, Yokohama National University

1. INTRODUCTION: Wind-induced structural instability is one of the most important problems both in design and construction of long-span cable-stayed bridges. Wind-induced instability of the long-span bridges is generally caused by one or the combinations of the following three behaviors: (1) aerostatic and aerodynamic phenomenons resulting in motion-dependent wind loads, (2) flexural-torsional buckling, and (3) material plasticity. The effects of displacement-dependent wind loads and geometric nonlinearity on the flexural-torsional buckling of this type of bridge were investigated by the authors [1]; however, the material plasticity was not considered in the previous investigation. In this study, second-order inelastic instability analysis under displacement-dependent wind loads is presented by a concentrated plasticity approach. For practical inelastic instability analysis of realistic structures, finite element methods using beam-column and truss elements with concentrated plastic hinge models appear to hold the most promise [2-5].

2. INELASTIC BEAM-COLUMN FORMULATION: Using the concentrated plastic hinge assumption, the inelastic beam-column element can be idealized as shown in Fig. 1. The element consists of an elastic portion of finite length and two rigid-plastic elements of zero length. The element tangent stiffness matrix $\mathbf{k}_t$ can be calculated by the following equation [3, 5]:

$$\mathbf{k}_t = \mathbf{k}_e + \mathbf{k}_g - \mathbf{k}_p \tag{1}$$

where $\mathbf{k}_e$ is the conventional linear elastic stiffness matrix; $\mathbf{k}_g$ is the geometric stiffness matrix that is used to model various elastic instabilities, such as, flexural, torsional, and flexural-torsional buckling [1]; $\mathbf{k}_p$ is the plastic reduction matrix to account for inelastic effects. As long as the element is fully elastic, $\mathbf{k}_p$ is of course a null matrix.

The elastic or inelastic of the element ends can be determined by the value of yield surface function. For a three-dimensional beam-column element with a symmetrical steel cross section, the yield surface can be practically expressed as

$$\Phi = \left[\left(\frac{M_x}{M_{px}}\right)^2 + \left(\frac{M_y}{M_{py}}\right)^2 + \left(\frac{M_z}{M_{pz}}\right)^2\right]^{1/2} + \left(\frac{F_x}{F_{px}}\right)^n - 1 = 0 \tag{2}$$

where M_X , M_Y and M_Z are the torsion and bending moments as shown in Fig. 1; F_X is the axial force; M_{px}, M_{py} and M_{pz} are the plastic torsion and bending moments; F_{px} is the plastic axial force; and the exponent n varies between 1.3 and 2 depending on the cross section. The value n = 1.6 considered to be sufficiently accuracy for practical application [2] is adopted in this study.

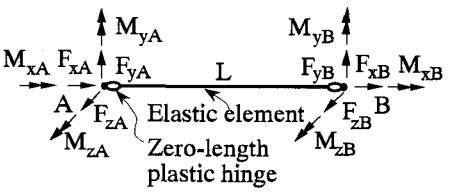

Fig. 1 Inelastic beam-column model

3. MODELING OF WIND-INDUCED INELASTIC INSTABILITY: The modeling of second-order inelastic instability under the displacement-dependent wind loads involves increment-iteration approach. The modeling is composed of a two-step process. In the first step process, nonlinear analysis under the initial wind loads of given wind velocity V is performed by incremental procedure. In the second step process, nonlinear analysis under the additional and unbalanced wind loads is performed by Newton-Raphson iterative procedure. The additional loads are induced by increasing angle of wind attack due to the torsional deformation of the deck, while the unbalanced loads are caused by the imbalance between external applied and internal resisting nodal loads. The linearized incremental equilibrium equation of the whole bridge subjected to the additional and unbalanced wind load vectors for jth iteration is written as

$$\left[\mathbf{K}_t^{G+W}\left(u_{j-1}, \sigma_{j-1}\right)\right]\Delta\mathbf{U}_j = \mathbf{F}_j\left(F_X(\alpha_j), F_Y(\alpha_j), M_Z(\alpha_j)\right) - \mathbf{R}_{j-1} \tag{3}$$

where $\mathbf{K}_t$ is the structural tangent stiffness matrix computed on the basis of the displacements u and stresses σ from the preceding iterations; superscripts G and W mean gravity and wind loads, respectively; $\Delta\mathbf{U}_j$ is the incremental displacement vector; $\mathbf{F}_j$ is the displacement-dependent wind load vectors (consisting of drag force F_X, lift force F_Y, and pitching moment M_Z) computed on the basis of the current wind angles of attack;

and $\mathbf{R}_{j-1}$ is the internal resisting nodal load vector computed on the basis of the displacements from the preceding iterations. The more detail can be found in reference 5.

4. BEHAVIOR OF INELASTIC INSTABILITY

A long-span cable-stayed bridge of a case study has a main span length of 1000 m and two 450 m side spans. The three-dimensional finite-element modeling of the completed bridge and the half-span bridge just before closing are shown in Figs. 2b and 2c. Yield stress for the cable is 14 tf/cm^2, and yield stress for the tower and deck is 3.5 tf/cm^2. The structural instability analysis was performed for the following loading sequence: (1) Dead loads of 26.5 tf/m and prestresses of cables are first applied, and (2) displacement-dependent wind loads are then applied until instability is reached.

In the completed bridge case (see Figs. 2a and 2b), the first and second hinges form in the lower strut of the left and right towers at wind velocity of 73 m/s. With relatively high axial force and bending moment at the leeward supports of both towers, fifth and sixth hinges then form at these locations at wind velocity of 110 m/s. After that, hinges occur in the deck near both left and right towers at wind velocity of 111 m/s. Finally, at wind velocity of 121 m/s, the inelastic instability at which the determinant of the effective tangent stiffness matrix of structure becomes zero or negative is reached. At this limit point, the axial stresses in all stay cables do not exceed the yield stress. Although a large number of hinges have formed in the towers and deck at this limit point, a kinematic mechanism in the classical approach does not exit. Therefore, the limit point is a result of both structural buckling (geometric) and plasticity (material) destabilizing effects.

In the half-span bridge case (see Figs. 2a and 2c), the inelastic instability occurs at wind velocity of 80 m/s. The effects of displacement-dependent wind loads on the half-span bridge are much more important than those on the completed bridge (see the slope of displacement). If the material plasticity is neglected in the analysis, the second-order elastic instability occurs at wind velocity of 123 m/s for the half-span bridge and 146 m/s for the completed bridges.

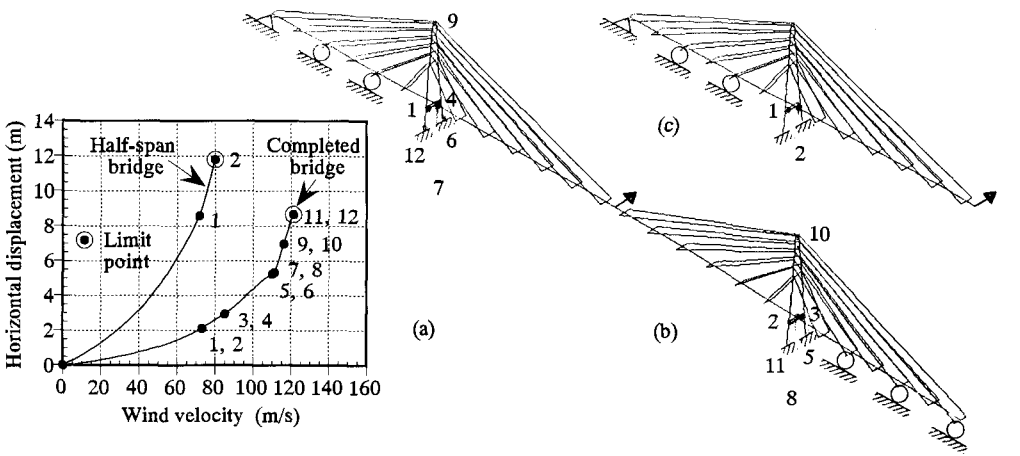

Fig. 2 (a) Horizontal displacement behavior at midpoint of main span and hinge formation sequence for: (b) completed bridge; and (c) half-span bridge

5. CONCLUSIONS: The concentrated plasticity approach to wind-induced second-order inelastic instability analysis of the long-span cable-stayed bridge was studied. The proposed method includes directly the effects of: (a) the three-component displacement-dependent wind loads, (b) structural buckling, and (c) material plasticity, in the analysis. The wind-induced instability of this type of bridge is caused by the combinations of these three effects. The half-span bridge during erection is much more susceptible to the inelastic instability than the completed bridge.

6. REFERENCES: [1] Boonyapinyo, V., Yamada, H., and Miyata, T., "Wind-induced nonlinear lateral-torsional buckling of cable-stayed bridges," *J. Struct. Engrg.*, ASCE, Vol. 120(2), pp. 486-506, 1994. [2] Powell, G.H., and Chen, P.F., "3D beam-column element with generalized plastic hinges," *J. Struct. Engrg.*, ASCE, Vol. 112(7), pp. 627-641, 1986. [3] Ziemian, R.D., McGuire, W., and Deierlein, G.G., "Inelastic limit states design part I & II," *J. Struct. Engrg.*, ASCE, Vol. 118(9), pp. 2532-2568, 1992. [4] Liew, J.Y.R., White, D. W., and Chen, W.F., "Second-order refined plastic-hinge analysis for frame design part I & II," *J. Struct. Engrg*, ASCE, Vol. 119(11), pp. 3196-3237, 1993. [5] Miyata, T., Yamada, H., and Boonyapinyo, V., "Importance of wind loads in buckling instability of super-long cable-stayed bridges," *Proc. of Int. Conf. on Cable-Stayed and Suspension Bridges*, Deauville, France, 1994 (Accepted).